Drop-Turbulence Interactions in a Diffusion Flame

J.-S. Shuen,* A.S.P. Solomon,† and G.M. Faeth‡
The Pennsylvania State University, University Park, Pennsylvania

An experimental and theoretical study of drop processes in a turbulent flame environment, having a known structure, is described. The experiments involved a monodisperse (105- or 180-μm initial diameter) stream of methanol drops injected along the axis of a turbulent methane-fueled diffusion flame burning in still air. The following measurements were made: mean and fluctuating phase velocities, mean drop number flux, drop size distributions, and mean gas-phase temperature. Measurements were compared with predictions of two separated flow analyses: 1) deterministic separated flow, where drop-turbulence interactions are ignored; and 2) stochastic separated flow, where drop-turbulence interactions are considered using random-walk computations. The stochastic separated flow analysis yielded best agreement with measurements, since it provides for turbulent dispersion of drops which was important for the test conditions, and probably for most combusting sprays. Distinguishing the presence or absence of envelope flames around the drops, however, was relatively unimportant for these test conditions, since the drops spent most of their lifetime in flow regions having low oxygen concentrations, where this distinction is irrelevant.

Nomenclature

d, d_P = injector and drop diameters, respectively
f = mixture fraction
g = square of mixture fraction fluctuations
k = turbulence kinetic energy
L = distance between drop generator and burner exit
n = number of drop groups
$\dot{n}''$ = drop number flux
pdf(f) = probability density function of f
Re = Reynolds number
r = radial distance
SMD = Sauter mean diameter
t = time
T = gas temperature
u, v, w = axial, radial, and tangential velocities, respectively
x = axial distance
α = weighting factor for property selection
ϵ = rate of dissipation of turbulence kinetic energy
θ = generic property
ρ = density
ϕ = fuel equivalence ratio

Subscripts

c = centerline quantity
P = drop property
s = drop surface
0 = burner exit condition
∞ = ambient condition

Supercripts

$(\bar{}), (\bar{})'$ = time-averaged mean and fluctuating quantities, respectively
$(\tilde{}), (\tilde{})''$ = Favre-averaged mean and fluctuating quantities, respectively

Received Nov. 16, 1984; presented as Paper 85-0319 at the AIAA 23rd Aerospace Sciences Meeting, Reno, NV, Jan. 14-17, 1985; revision received May 6, 1985.

*Research Assistant, Department of Mechanical Engineering; currently, Senior Research Engineer, Sverdrup Technology Inc., Cleveland, OH.

†Research Assistant, Department of Mechanical Engineering; currently, Senior Research Engineer, General Motors Research Laboratories, Warren, MI.

‡Professor of Mechanical Engineering; currently, Professor of Aerospace Engineering, University of Michigan, Ann Arbor, MI. Associate Fellow AIAA.

Introduction

THIS study is an extension of earlier work at The Pennsylvania State University (PSU) on the structure of turbulent particle-laden jets,[1-3] nonevaporating sprays,[4,5] and evaporating sprays.[6] The objective was to initiate consideration of combusting sprays by studying the properties of widely separated drops in a turbulent diffusion-flame environment. Emphasis was placed on drop-turbulence interactions, e.g., turbulent dispersion of drops, effects of turbulent fluctuations on interphase transport rates, and effects of the presence or absence of envelope flames around individual drops.

Past work on spray flames was recently reviewed by one of the present authors and this discussion will not be repeated here.[7] It was found that little data exist concerning the transport properties of freely moving drops in turbulent diffusion-flame environments. There is a particular need for studies in well-characterized flame environments that can provide information on drop-turbulence interactions.

These experimental objectives were met by injecting a monodisperse stream of drops into the base of a turbulent methane-fueled diffusion flame burning in still air. The flow was lightly loaded with drops; therefore, the flame structure was controlled by methane combustion and was known from earlier work at PSU.[8,9] Drop properties could also be measured with reasonable reliability, since drop concentrations were small, which avoids instrumentation problems encountered in dense (high-liquid-fraction) sprays.[7]

The experiments were analyzed to help interpret the measurements and develop spray analysis methods. Two methods were studied: 1) deterministic separated flow (DSF) analysis, where effects of drop-turbulence interactions were ignored; and 2) stochastic separated flow (SSF) analysis, where drop-turbulence interactions were considered using random-walk computations for drop motion and transport. The former method is typical of most current spray analyses.[7] The latter method is based on an original proposal by Gosman and Ioannides,[10] which yielded encouraging results during subsequent development at PSU.[1-6] The effect of envelope flames around individual drops when they contact oxygen-containing regions in a turbulent flame environment was also studied. This involved calculations both considering and ignoring the presence of envelope flames. Analysis of single-drop transport was calibrated using data from drops supported in the postflame region of a laminar flat-flame burner.

In the following, experimental and theoretical methods are described first. Baseline results for single-drop transport calibrations and diffusion-flame structures are then considered. The paper concludes with a discussion of findings for the spray-flame tests. The present discussion is brief, full details and tables of data appear elsewhere.[11]

Experimental Methods

Test Arrangement

The basic test arrangement was originally used by Jeng and co-workers[8,9] to study methane diffusion flames. The burner flow was injected vertically upward within a screened enclosure while combustion products were removed at the test cell ceiling. Rigidly mounted optical instruments were used for some measurements; therefore, the entire cage assembly was traversed to measure radial profiles.

The burner both stabilized the flame and injected a monodisperse stream of drops into the flow. Methanol was used for the drops, since it has a relatively slow rate of vaporization which extended the multiphase-flow region. Natural gas (more than 95% methane) was used to fuel the diffusion flame.

Figure 1 is a sketch of the burner. The drops were formed using a commercial vibrating-orifice Berglund-Liu monodisperse drop generator (TSI model 3050). This generates a stream of drops partly spread by a dispersing gas flow (which was methane). The methane diffusion flame was attached at the burner exit using a small annular coflow of hydrogen. The top of the burner was water-cooled to room temperature, which minimized effects of extraneous natural convection flows.

Test Conditions

Test conditions are summarized in Table 1. The methane diffusion flame was identical to the highest Reynolds number flame considered by Jeng and co-workers.[8,9] The flame height (mean fuel equivalence ratio of unity at the axis) was roughly 600 mm. Two drop sizes were studied having initial diameters of 105 and 108 μm. Liquid flow rates were small; therefore, the drop stream had little effect on flame structure.

Instrumentation

Phase Velocities

Mean and fluctuating phase velocities were measured using a single-channel laser Doppler anemometer (LDA), similar to past work.[1-6] Several beam orientations provided various velocity components, while frequency shifting eliminated errors due to fringe bias and flow reversals. The measuring volume had diameters and lengths of 100, 200 μm ($x/d=1$) and 247, 720 μm ($x/d>1$).

Continuous-phase velocities were measured by seeding both burner and ambient gases (to avoid concentration bias) with 500-nm-diam aluminum oxide particles, with no drops present. Seeding levels were sufficiently high so that time-averaged velocities could be obtained with little velocity bias. Combined errors of gradient broadening, beam steering, phase fluctuations, and processing yield less than 5% uncertainties in mean and fluctuating gas velocities and less than 10% uncertainty in turbulence kinetic energy.

Drop velocities were measured with no seeding particles present and reduced detector gain so that only relatively strong LDA signals from drops were processed. Local drop size variations were not large (except at positions near the end of drop life); therefore, drop size and velocity correlations were not attempted. This was acceptable for evaluation of analysis since computed properties could easily be averaged over all sizes at a point. The data were obtained as number averages for direct comparison with analysis. Uncertainties in gas and drop velocity measurements were similar.

Drop Size Distributions

Drop size distributions were measured using slide impaction, similar to past work.[4-6] Since drop sizes were relatively uniform, only 200 drops had to be counted to obtain the Sauter mean diameter (SMD) within a 10% uncertainty. SMD was only measured down to 30 μm; therefore, impactor collection efficiencies were essentially 100% for present conditions.

Drop Number Fluxes

Drop number fluxes were measured using Mie scattering from a laser light sheet. The beam from a 50-mW HeNe laser was spread using a cylindrical lens system and passed through the flame. A small section of the sheet was observed with a detector through a laser-line filter and collecting optics. Light pulses generated by drops passing through the measuring volume were processed using a pulse counter. The region observed varied with drop size and was calibrated using a range of settings on the drop generator. The maximum cross-sectional area of observation was for 180-μm-diam drops (0.2 mm^2 for $x/d\geq 12$, 2.9 mm^2 for $x/d>12$). The raw data were corrected to account for the size effect, but the correction was not large since the drop size range was generally narrow at each point. Estimated uncertainty of these measurements due to the calibration, sampling, and processing errors was less than 15%.

Mean Gas Temperatures

Mean gas temperatures were measured with no drops present, using a butt-welded Pt/Pt-10% Rh thermocouple constructed of 75-μm-diam wires. Indicated temperatures were corrected for radiation errors similar to past practice.[9] Probe output was recorded with a minicomputer to yield time

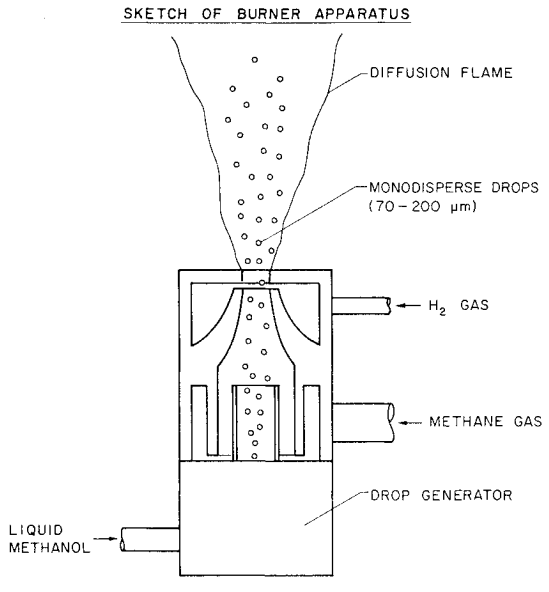

Fig. 1 Burner assembly.

Table 1 Test conditions[a]

Nominal drop diameter, μm	105	180
Liquid volume flow rate,[b] μl/s	12.21	24.48
Generator frequency, kHz	20	7.96
Generator orifice diameter, μm	50	100

[a]Natural gas and hydrogen flow rates of 520 and 14.6 mg/s; burner exit diameter of 5 mm; initial Reynolds number of 11,700; initial centerline velocity ($x/d=1$) of 52.8 m/s; ambient temperature and pressure of 300 ± 2 K and 97 kPa.
[b]Methanol (laboratory grade).

averages. Uncertainties are estimated to be less than 5% of the local temperature difference between the gas and the surroundings.

Theoretical Methods

Continuous Phase

Flame structure was not appreciably influenced by the drops; therefore, source terms due to drops in the continuous-phase governing equations could be ignored with little error. As a result, the continuous phase was analyzed using the methods of Jeng and Faeth,[9] since their approach yielded satisfactory structure predictions for virtually the same flame.

Major assumptions of the continuous-phase analysis were: boundary-layer approximations apply for an axisymmetric flow with no swirl, exchange coefficients of all species and heat are the same, buoyancy only affects the mean flow, and kinetic energy of the mean flow is negligible. The Favre-averaged formulation of Bilger[12] was adopted. The conserved-scalar formalism was used to find scalar properties. This involves solving governing equations for mean conservation of mass, momentum, and mixture fraction. Turbulence closure was achieved by solving modeled governing equations for k, ϵ, and g, with all model constants fixed by measurements in constant- and variable-density noncombusting jets.[9]

Scalar properties were found from the probability density function of mixture fraction, pdf(f), in conjunction with state relationships giving scalar properties as a function of mixture fraction. A clipped Gaussian function was used for this pdf, with its two parameters found from the known local values of $\tilde{f}$ and g as described by Lockwood and Naguib.[13] State relationships were prescribed using the laminar flamelet technique of Bilger[14] and Liew et al.[15] This involves correlating scalar property measurements in laminar diffusion flames. A nearly universal correlation is found, independent of local flame conditions; therefore, this correlation is used for the turbulent flame calculations, assuming that properties therein result from a succession of laminar flamelets passing a given location, cf. Jeng and Faeth[9] for details. This procedure partially compensates for flame radiative heat losses, as long as the laminar and turbulent flames are optically thin—which was roughly true for present conditions.

Dispersed Phase

Drop Transport

The dispersed phase was treated by solving Lagrangian equations of motion and transport for the trajectories of a statistically significant sample of drops; dividing the drops into n groups (defined by initial position and velocity) at the burner exit and computing their subsequent life histories in the flow. Major assumptions of the drop trajectory calculations were: drop transport equivalent to a single drop in an infinite environment, empirical treatment of drag and convection effects, quasisteady gas phase, liquid surface in thermodynamic equilibrium, negligible drop shattering and collisions, negligible effects of radiation, only concentration diffusion with equal binary diffusivities for all species, and constant average transport properties at each instant. These assumptions are common to most drop-life history and spray calculations; their justification is discussed elsewhere.[7]

Consideration of energy transport within drops unduly complicates analysis; therefore, the thin-skin approximation was used. This implies that the bulk liquid remains at its initial condition while only an infinitely thin layer at the surface is heated during evaporation. This approximation yields results for transient drop effects which are comparable to the more widely used uniform drop temperature approximation.[7]

During their motion through the flow, drops approach and penetrate the reaction (flame) zone of the methane diffusion flame itself, encountering regions where oxygen is present in a relatively high-temperature gas. Specification of drop ignition is not well understood for diffusion-flame environments; therefore, two limits were examined: 1) no ignition in all regions of the flow, and 2) ignition with an envelope flame surrounding the drop whenever the local environment contains oxygen. The specific formulation for transport in each case and a summary of drag and convection empirical parameters are presented elsewhere.[7,11]

Drop-Life-History Calibrations

It is well-known that a priori calculations of drop-life histories are very uncertain when using constant-property models, due to the large variation of properties in the drop flowfield. In order to reduce this uncertainty, calibration tests were undertaken in the postflame region of a laminar flat-flame burner. Measurements and computations for these tests were matched by selecting the optimum weighting parameter α to define the property reference state

$$\theta_{\text{avg}} = \alpha\theta_s + (1-\alpha)\theta_\infty \tag{1}$$

where θ is a generic quantity representing either a species mass fraction or temperature.

The calibration tests were conducted using the flat-flame burner apparatus of Szekely and Faeth.[16] The drops were supported on a quartz fiber and rapidly immersed in the postflame region. The drops were backlighted and photographed with timing marks placed on the motion-picture film. Processing the photographs with an image analyzer then yielded drop sizes as a function of time. Gas properties at the drop location were found as follows: gas composition by sampling and analysis with a gas chromatograph; gas temperature using a radiation-corrected thermocouple similar to the turbulent flame tests, and gas velocities by computation, knowing the burner flow rate and cross-sectional area as well as the gas properties.

Test conditions for the drop-life-history calibrations are summarized in Table 2. Flame conditions are characterized by the fuel equivalence ratio. Drop diameters were large in comparison to the turbulent flame tests, however, Reynolds numbers are comparable due to the low velocities in the laminar flat-flame burner. Methane-air mixtures were used to fuel the burner so that conditions were representative of the turbulent flame.

Predicted and measured drop-life histories are illustrated in Fig. 2. Predictions are shown for the limiting cases of envelope flames present or absent—both for the matched condition choosing $\alpha = 0.3$ in Eq. (1). Envelope flames were observed for these conditions and the results are matched accordingly. The distinction is not very large for $\phi = 0.97$ (and, of course, is inconsequential for fuel equivalence ratios greater than unity). The comparison between predictions and measurements is excellent, providing some confidence in individual drop-life-history computations.

Deterministic Separated Flow Analysis

The most stringent assumption of this approximation is that drop transport and motion are computed using mean proper-

Table 2 Summary of drop-life-history test conditions[a]

Fuel equivalence ratio	0.65	0.82	0.97
Initial drop diameter, μm	2293	2786	2953
Gas temperature, K	1500	1690	1690
Gas mass fractions			
O_2	0.076	0.038	0.000
N_2	0.755	0.744	0.778
H_2O	0.077	0.098	0.099
CO	0.004	0.000	0.001
CO_2	0.088	0.120	0.122
Initial drop *Re*	19	21	28

[a] Methanol drops supported in the postflame region of a flat-flame burner fueled with methane-air mixtures.

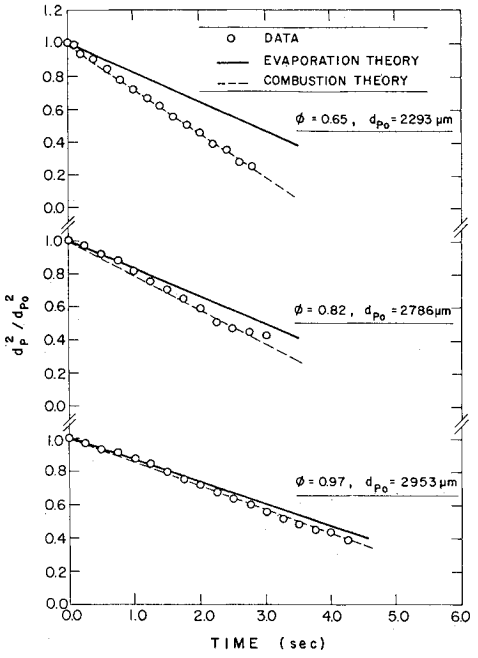

Fig. 2 Drop-life-history calibrations.

ties estimated from the continuous-phase analysis. As a result, drop-turbulence interactions are ignored and drops follow deterministic trajectories based on their location and velocity at the burner exit. Trajectories of 1200 drops were computed in order to obtain a statistically significant representation of the flow.

Time-averaged gas properties should be used in drop trajectory calculations. Following Bilger,[12] time-averaged scalar properties can be found directly from the conserved-scalar approach. Favre-averaged velocities are computed, however, and cannot be converted into time-averaged velocities without extension of the analysis to find correlations of density-velocity fluctuations. Therefore, Favre-averaged velocities were used in the calculations. Fortunately, differences between Favre- and time-averaged velocities are estimated to be less than 5% in the test flame (although differences between these averages for scalar properties can be much larger).[9]

Stochastic Separated Flow Analysis

With this approach, drops are assumed to interact with a succession of eddies as they move through the flow. Properties within a particular eddy are assumed to be uniform, but properties change in a random fashion from eddy to eddy. The trajectory calculations are the same as in the DSF analysis, except that instantaneous eddy properties are used rather than mean properties.

The properties of each eddy at the start of drop-eddy interaction were found by making a random selection from the pdf's of velocity and mixture fraction, assuming that these properties are statistically independent. The velocity fluctuations were assumed to be isotropic with a Gaussian pdf having a most probable value found from the local mean velocity and a variance of $2k/3$—both obtained from the continuous-phase solution. The distinction between the Favre- and time-averaged velocities was ignored, similar to the DSF analysis.

Scalar properties of the eddy were found by converting the Favre-averaged pdf(f) to a time-averaged pdf,[9] following Bilger.[12] The time-averaged pdf was randomly sampled to get an instantaneous value of f. Scalar eddy properties for this f were then obtained directly from the state relationships.

A drop was assumed to interact with an eddy for a time that is the minimum of either the eddy lifetime or the transit time required for the drop to cross the eddy. These times are found

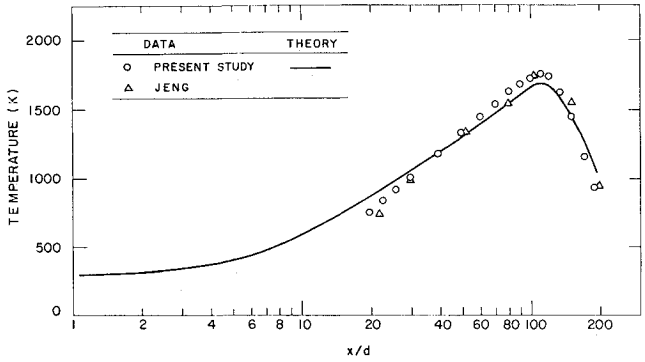

Fig. 3 Mean gas temperatures along the axis.

using the local dissipation length scale and k; information that is directly available from the continuous-phase analysis.[1-6]

The SSF analysis requires more drop trajectories than the DSF analysis to obtain statistically significant results, e.g., 6000 trajectories for the present results. However, the approach does provide both mean and fluctuating drop properties in the flow for comparison with the measurements.

Results and Discussion

Initial Conditions

Initial conditions were measured one injector diameter beyond the burner exit. Continuous-phase measurements included: mean streamwise velocity and all three components of velocity fluctuations (yielding k). The measured rate of decay of k and the value of $\bar{u}$ in the potential core yielded ϵ. At the exit, $\tilde{f}=1$ and $g=0$ by definition; completing specification of gas-phase properties.

Drop diameters were constant and mean and fluctuating streamwise velocities as well as fluctuating radial velocities of drops were measured at the burner exit. The drop number flux distribution was also measured. Radial mean drop velocity could not be measured accurately since it is small; therefore, it was estimated assuming $\bar{v}_p = \bar{u}_p r/L$, where r is the radial position and L the distance between the vibrating orifice of the drop generator and the burner exit. Only mean values were used to fix initial velocities for the DSF analysis, however, the measured drop velocity pdf's were sampled directly for SSF computations.

Mean Gas Temperatures

Maximum differences between the Favre- and time-averaged temperatures are less than 200 K in the flame, and smaller elsewhere, while thermocouples generally yield values between the two.[9] Therefore, predicted Favre-averaged mean gas temperatures along the axis are plotted along with the measurements in Fig. 3. Present measurements are shown along with the earlier results of Jeng and Faeth[9] for the same flame (aside from the presence of the drop generator in the burner). Both sets of measurements are virtually identical, indicating excellent reproducibility of the earlier work. Predictions are in good agreement with measurements, indicating that the analysis provides a reasonably good estimation of mean scalar properties, cf. Ref. 9 for comparisons of other mean scalar properties.

Mean Phase Velocities

Mean gas (time-averaged) and drop (particle-averaged) velocities along the axis are illustrated in Fig. 4. Drop velocities for both sprays are shown along with SSF predictions. As noted earlier, predicted gas velocities are Favre averages, while predicted drop velocities are particle averages for direct comparison with measurements. Gas velocities are substantially greater than drop velocities at the burner exit;

however, they decrease rapidly due to mixing with the surroundings. Near the injector, the drops have significant inertia and their velocities only gradually increase in response to the higher gas velocities. Near the tip of the flame (maximum temperature location at about $x/d = 120$, cf. Fig. 3), however, drop sizes are small and their velocities approach gas velocities. Drops in both sprays penetrate beyond the flame tip; therefore, the presence or absence of envelope flames should be a factor. This was found to have little effect on present computations, however, and predictions are only illustrated neglecting the presence of envelope flames.

Radial profiles of mean phase velocities are illustrated in Fig. 5. The abscissa of this plot, and all other radial profile illustrations, is r/x, so that estimates of flow width can be directly assessed. Slip between the phases is most important for large drops near the injector and becomes small near the flame tip. Drop velocity measurements could be undertaken only where reasonable numbers of drops were present, this region is roughly bounded by the flame zone where drop vaporization rates are high.

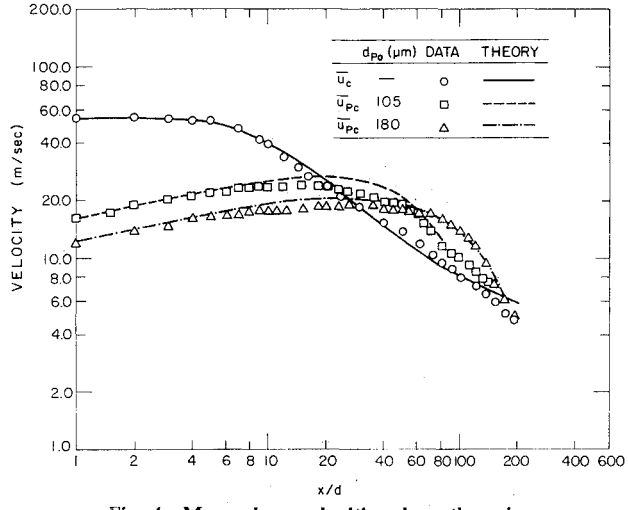

Fig. 4 Mean phase velocities along the axis.

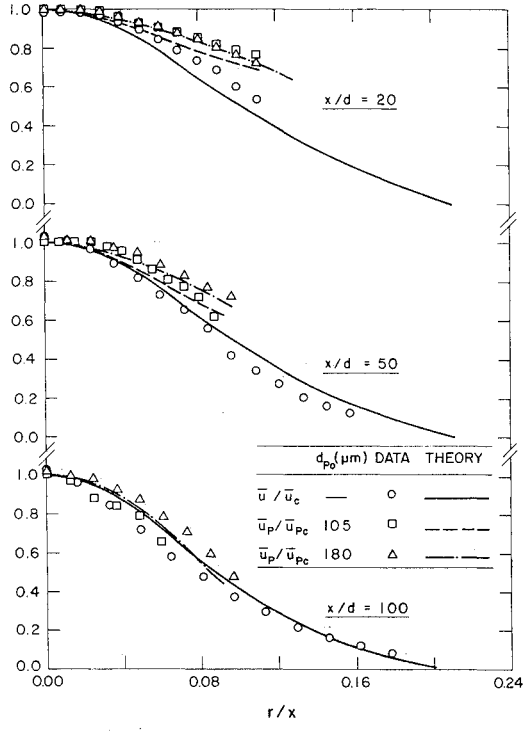

Fig. 5 Radial profiles of mean phase velocities. (Drop property predictions are from SSF model.)

Fluctuating Phase Velocities

Predicted and measured phase velocity fluctuations along the axis are illustrated in Fig. 6. Predicted gas velocity fluctuations were computed using the anisotropy levels generally associated with jets and observed in the present flame, e.g., $\tilde{u}''^2 : \tilde{v}''^2 : \tilde{w}''^2 = k : k/2 : k/2$, while predictions for the drop phase were found directly from the SSF analysis (drop velocity fluctuations were averaged over all drop sizes present at each point, which corresponds to the measurements). As noted earlier, gas-phase predictions are Favre averages while the measurements were time averages, however, this distinction is comparable to experimental uncertainties.[9]

Gas-phase turbulence intensities seen in Fig. 6, at the burner exit, were higher than the observations of Jeng and Faeth,[9] probably due to additional disturbances resulting from the presence of drop generator components within the burner. Predicted gas velocity fluctuations are generally within 20% of

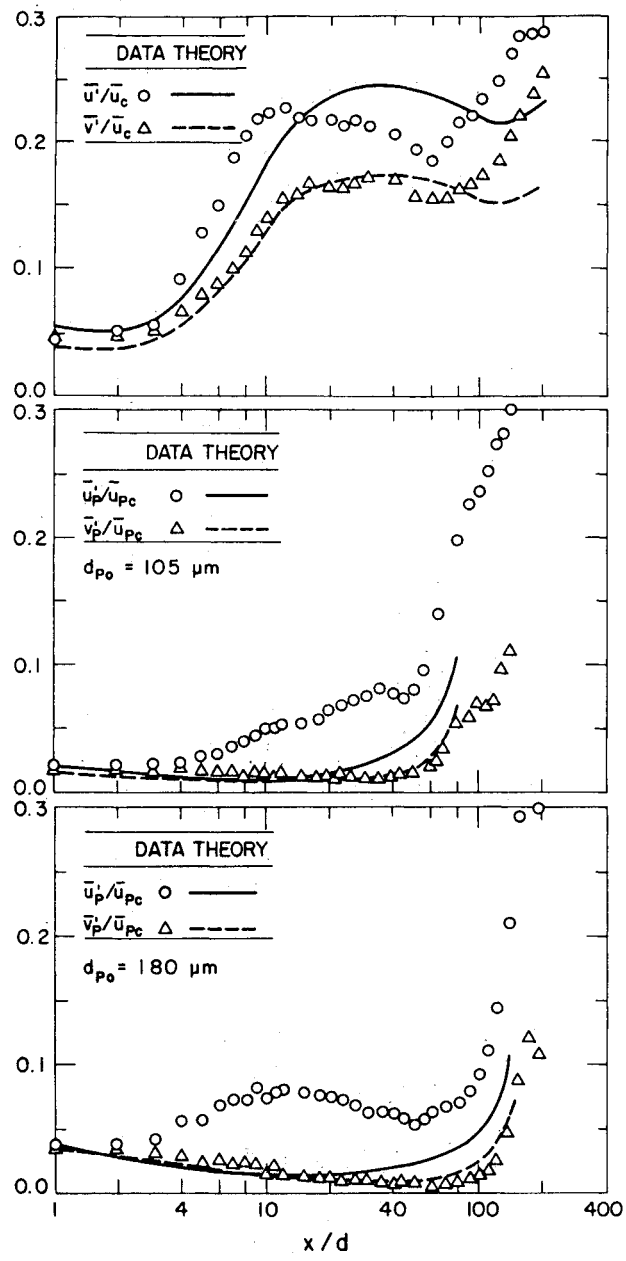

Fig. 6 Fluctuating phase velocities along the axis. (Drop property predictions are from SSF model.)

the measurements, which is reasonably good in view of the relative simplicity of the continuous-phase analysis. Radial drop velocity fluctuations are also predicted reasonably well, which is important if turbulent dispersion of drops is to be represented accurately. Streamwise drop velocity fluctuations are underestimated, however, similar to past performance of the SSF analysis.[3-6] This is probably due to the assumption of isotropic eddy properties when the drop-eddy interaction is prescribed. Extension of the SSF analysis to consider anisotropy would be desirable. Near the burner exit, drop velocity fluctuations are small in comparison to the gas phase, due to drop inertia. However, at the end of drop lifetime (near the flame tip), the remaining small drops can respond rapidly and approach velocity fluctuation levels of the continuous phase.

Predicted and measured radial profiles of gas and drop velocity fluctuations are illustrated in Figs. 7-9. The DSF model provides no information on the fluctuating properties of drops; therefore, only SSF predictions are shown in Figs. 8 and 9. Comparison between predictions and measurements is reasonably good, except that streamwise drop velocity fluctuations are underestimated by predictions, as noted earlier. Another defect is that drops having an initial diameter of 105 μm were predicted to disappear prior to $x/d = 100$; therefore, no predictions could be made for this position even though the measurements show that drops were present. Gas velocity fluctuations tend to decrease in the radial direction, typical of jets and jet flames.[8,9] Drop velocity fluctuations increase, however, since the drops are smaller and more responsive near the edge of the two-phase flow region.

Drop Number Flux

Predicted and measured mean drop number fluxes (both time averages) along the axis are illustrated in Fig. 10. Predictions of both the SSF and DSF analyses are shown. The SSF analysis is in quite good agreement with the measurements, except for a tendency to underestimate drop number fluxes near the flame tip. In contrast, the DSF analysis overestimates drop number fluxes along the axis, since this approach ignores turbulent dispersion of drops which is clearly important for the present conditions. With the DSF approach, drops only move radially due to their initial mean radial velocity and the drag on them from the mean radial velocity of the continuous phase—both of which are small in comparison to radial velocity fluctuations.

Predicted and measured radial profiles of mean drop number fluxes are illustrated in Fig. 11. Predictions are shown for both the DSF and SSF analyses, the former exhibiting poor comparison with measurements due to neglect of turbulent drop dispersion as noted earlier. The SSF analysis somewhat underestimates the radial spread of the drops,

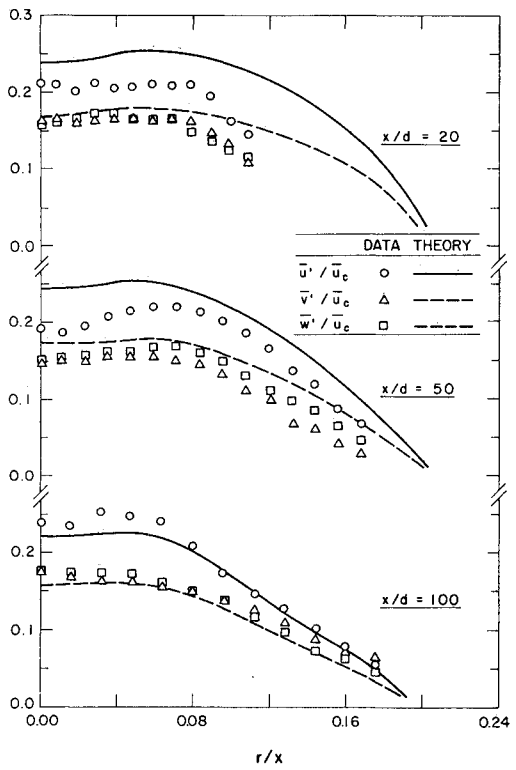

Fig. 7 Radial profiles of gas velocity fluctuations.

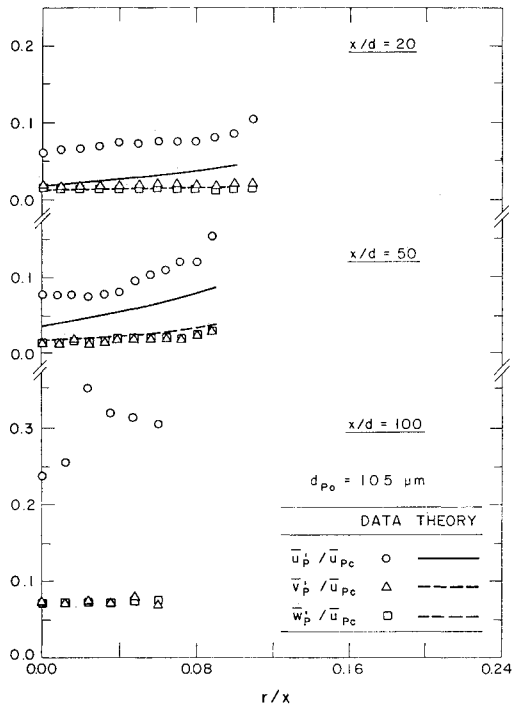

Fig. 8 Radial profiles of drop velocity fluctuations: $d_{p0} = 105$ μm. (Predictions are from SSF model.)

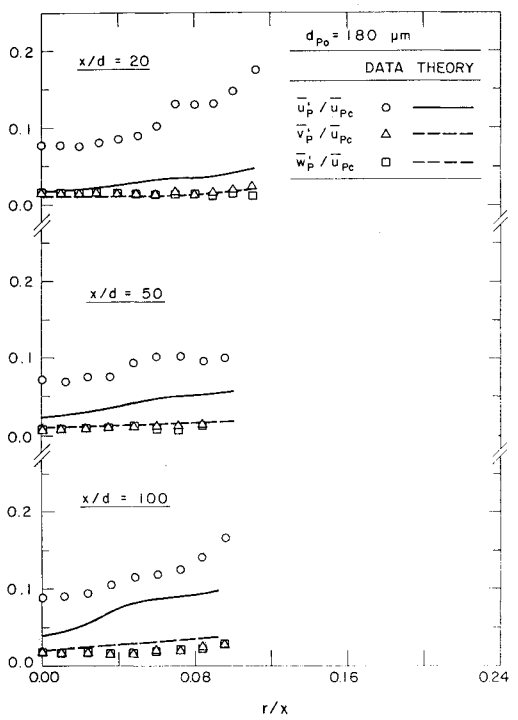

Fig. 9 Radial profiles of drop velocity fluctuations: $d_{p0} = 180$ μm. (Predictions are from SSF model.)

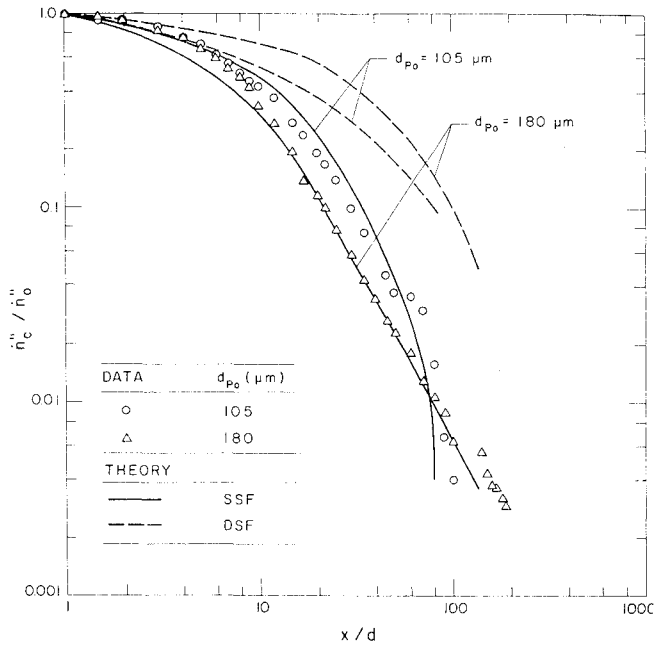

Fig. 10 Mean drop number flux along the axis.

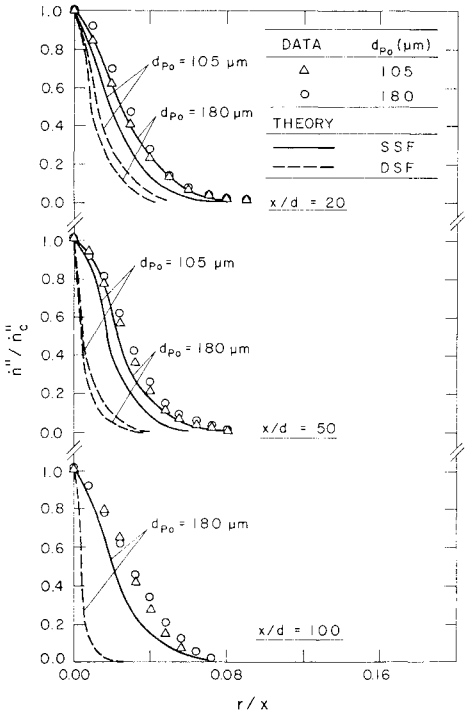

Fig. 11 Radial profiles of drop number flux.

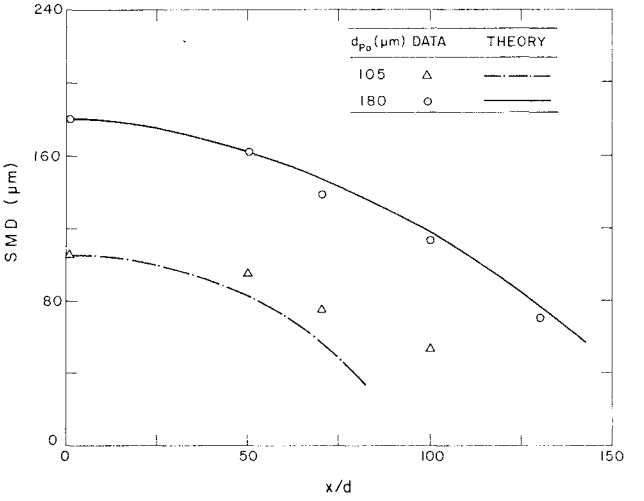

Fig. 12 SMD along the axis. (Predictions are from SSF model.)

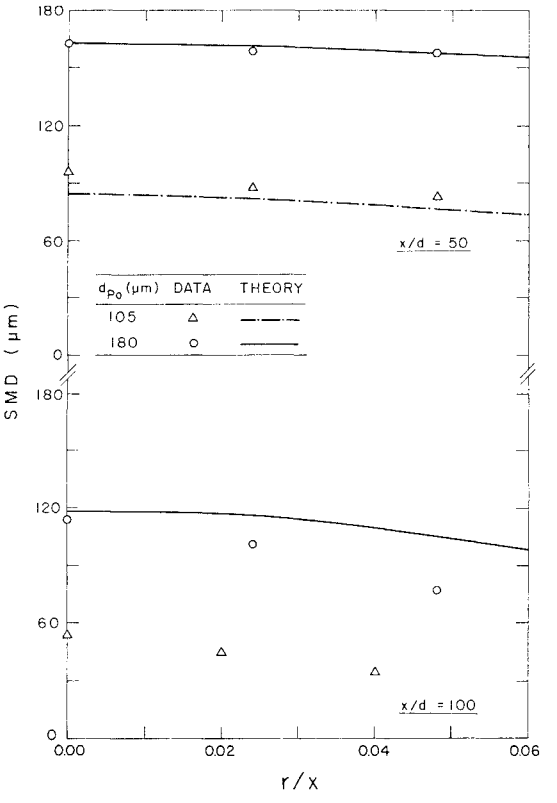

Fig. 13 Radial profiles of SMD. (Predictions are from SSF model.)

similar to its underestimation of streamwise drop penetration which was noted earlier. Mean drop velocities and radial drop velocity fluctuations are estimated reasonably well; therefore, this behavior is probably not due to underestimation of turbulent dispersion. Since both the length and width of the two-phase flow region were underestimated, a more probable source of error is overestimation of drop gasification rates in the flame zone.

Drop Size

Predicted (SSF analysis) and measured SMD along the axis are illustrated in Fig. 12. For the present initially monodisperse sprays, SMD decreases monotonically with increasing distance from the burner exit. Generally, this is not observed for polydisperse sprays, where more rapid evaporation and turbulent dispersion of small drops generally cause SMD to increase for a time along the axis.[4-6] Agreement between predictions and measurements is good for the 180-μm spray, but measurements are underestimated near the tip of the 105-μm spray, as noted earlier.

Predicted (SSF analysis) and measured radial profiles of SMD are illustrated in Fig. 13. Predictions are satisfactory at $x/d = 50$. However, at $x/d = 100$, drop sizes are overestimated for the 180-μm spray, while no drops are computed to be present for the 105-μm spray in spite of observations to the contrary. It appears that current methods need further examination in the flame region.

Conclusions

The present measurements should be useful for evaluating models of dilute sprays. The flow involves well-defined initial

and boundary conditions, extensive information is available on the structure of the test flame, and results are available to calibrate drop transport analysis. Test conditions were chosen to provide significant effects of finite interphase transport rates, turbulent dispersion of drops, and drop interactions with the flame zone. All structure measurements as well as properties at the burner exit are tabulated in Ref. 11.

Major conclusions of the study are as follows:

1) The DSF analysis, ignoring drop-turbulence interactions, was not very successful for the present flows. The main defect was significant underestimation of drop spread rates due to neglect of turbulent dispersion. In spite of its current popularity,[7] this approach appears to have limited value for analyzing practical combusting sprays.

2) The SSF analysis gave encouraging predictions of current results, with all empirical parameters either fixed during earlier work with noncombusting jets or calibrated by independent drop-life-history measurements. The largest discrepancies involved streamwise drop velocity fluctuations, which were underestimated similar to earlier work,[1-6] and transport rates of small drops in the flame zone, which were overestimated. Extension of current methods to consider anisotropic continuous-phase turbulence properties and further study of drop transport in flames appear to be warranted.

3) The distinction between the presence or absence of envelope flames did not modify present predictions appreciably, since drops primarily evaporated in the core of the flow where oxygen concentrations are low.[8,9] Further study of envelope flame effects is needed, however, since this may not always be the case and drops penetrated the flame zone for present test conditions, and probably do in practical flames as well.

4) The present experiment proved to be convenient for studying drop transport and dispersion in turbulent flames. The parabolic flow is attractive for numerically closed computations, initial conditions are readily measured, and flow properties are conducive to reasonably reliable measurements. Newly available methods for simultaneous drop size and velocity measurements could be fruitfully exploited in this flow.

Acknowledgments

This research was sponsored by the National Aeronautics and Space Administration, Grant NAG 3-190, under the technical management of R. Tacina of the Lewis Research Center.

References

[1]Shuen, J.-S., Chen, L.-D., and Faeth, G.M., "Evaluation of a Stochastic Model of Particle Dispersion in a Turbulent Round Jet," *AIChE Journal*, Vol. 29, Jan. 1983, pp. 167-170.

[2]Shuen, J.-S., Chen, L.-D., and Faeth, G.M., "Predictions of the Structure of Turbulent, Particle-Laden Round Jets," *AIAA Journal*, Vol. 21, Nov. 1983, pp. 1483-1484.

[3]Shuen, J.-S., Solomon, A.S.P., Zhang, Q.-F., and Faeth, G.M., "Structure of Particle-Laden Jets: Predictions and Measurements," *AIAA Journal*, Vol. 23, March 1985, pp. 396-404.

[4]Solomon, A.S.P., Shuen, J.-S., Zhang, Q.-F., and Faeth, G.M., "Structure of Nonevaporating Sprays: I. Near-Injector Conditions and Mean Properties," *AIAA Journal*, Vol. 23, Oct. 1985, pp. 1548-1555.

[5]Solomon, A.S.P., Shuen, J.-S., Zhang, Q.-F., and Faeth, G.M., "Structure of Nonevaporating Sprays: II. Drop and Turbulence Properties," *AIAA Journal*, Vol. 23, Nov. 1985, pp. 1724-1730.

[6]Solomon, A.S.P., Shuen, J.-S., Zhang, Q.-F., and Faeth, G.M., "Measurements and Predictions of the Structure of Evaporating Sprays," *Journal of Heat Transfer*, Vol. 107, Aug. 1985, pp. 679-686.

[7]Faeth, G.M., "Evaporation and Combustion of Sprays," *Progress in Energy and Combustion Science*, Vol. 9, Jan. 1983, pp. 1-76.

[8]Jeng, S.-M., Chen, L.-D., and Faeth, G.M., "The Structure of Buoyant Methane and Propane Diffusion Flames," *Nineteenth Symposium (International) on Combustion*, The Combustion Institute, Pittsburgh, PA, 1982, pp. 1077-1085.

[9]Jeng, S.-M. and Faeth, G.M., "Species Concentrations and Turbulence Properties in Buoyant Methane Diffusion Flames," *Journal of Heat Transfer*, Vol. 106, Nov. 1984, pp. 721-727.

[10]Gosman, A.D. and Ioannides, E., "Aspects of Computer Simulation of Liquid-Fueled Combustors," AIAA Paper 81-0323, 1981.

[11]Shuen, J.-S., Solomon, A.S.P., and Faeth, G.M., "Structure of Dilute Combusting Sprays," NASA CR 174838, 1985.

[12]Bilger, R.W., "Turbulent Jet Diffusion Flames," *Progress in Energy and Combustion Science*, Vol. 1, Jan. 1976, pp. 87-109.

[13]Lockwood, F.C. and Naguib, A.S., "The Prediction of the Fluctuations in the Properties of Free, Round-Jet, Turbulent, Diffusion Flames," *Combustion and Flame*, Vol. 24, Aug. 1975, pp. 109-124.

[14]Bilger, R.W., "Reaction Rates in Diffusion Flames," *Combustion and Flame*, Vol. 30, 1977, pp. 277-284.

[15]Liew, S.K., Bray, K.N.C., and Moss, J.B., "A Flamelet Model of Turbulent Non-Premixed Combustion," *Combustion Science and Technology*, Vol. 27, Dec. 1981, pp. 69-73.

[16]Szekely, G.A. Jr. and Faeth, G.M., "Effects of Envelope Flames on Drop Gasification Rates in Turbulent Diffusion Flames," *Combustion and Flame*, Vol 49, Jan. 1983, pp. 255-259.